

The replacement reflection of a transition metal $3d^3$ by $3d^7$ on 4a site in Mn_2PtZ compounds: FP-LAPW approach

M Hamli^{1,5}, D Bensaid^{1,5*}, N Bouzouira², M Dine el Hannani¹, Y Azzaz³ and B Doumi⁴

¹Faculty of Sciences and Technology, University Belhadj Bouchaib, BP 284, 46000 Ain-Temouchent, Algeria

²University Centre Nour Bachir El Bayadh, El Bayadh, Algeria

³Faculty of Sciences, Djillali Liabes University of Sidi Bel-Abbes, 22000 Sidi Bel-Abbes, Algeria

⁴Faculty of Sciences, Department of Physics, Dr. Tahar, Moulay University of Saïda, 20000 Saïda, Algeria

⁵Laboratory Physico-Chemistry of Advanced Materials, University of Djillali Liabes, 22000 Sidi-Bel-Abbes, Algeria

Received: 07 November 2020 / Accepted: 25 March 2021

Abstract: We perform a first-principles calculation to understand the effect of the additional valence electron of the transition atom in Wyckoff position 4 a, on the electronic structure, magnetic and structural stability of the full Heusler Mn_2PtZ ($Z = \text{VandCo}$) compound. $L2_1$, Xa and tetragonal structures are considered to verify the most stable phase. Within the framework of the plan Mn_2PtZ ($Z = \text{VandCo}$) favored the ferromagnetic configuration in the $L2_1$ structure. The results show that the 63% and 91% spin polarization at the Fermi level for Mn_2PtV and Mn_2PtCo , respectively. The most contribution of the magnetic moment is due to the Mn atom, the total magnetic moments equal to $4.87\mu_B$ and $9.012\mu_B$ have been reported. To prove the half metallicity of our compound, we used the GGA + U approach. Within the framework of this approach, the value gap in the minority spin band is 0.755 eV, more, the magnetic moment satisfying the Slater-Pauling rule for the Mn_2PtV compound. In addition, we give the two values of the curie temperatures for the two cubic structural phases. Finally, both full Heusler Mn_2PtV and Mn_2PtCo are a promising candidate for the use of future devices as spin-FETs and nonvolatile magnetic memory.

Keywords: Heusler compounds; Half metallicity; DFT calculation; GGA + U approach; Electronic and magnetic properties

1. Introduction

The manganese-rich Heusler compounds have attracted attention in recent years due to its diversity in spintronic applications, as it displays a variety of fundamental physical phenomena of vital importance. They are used in spin-injection devices [1], spin-filters [2], electrodes for magnetic tunnel junctions (MTJs) [3], or GMR devices [4, 5] and for injection of spins into semiconductors [6]. The spintronic devices require the antiferromagnetic compounds, which are the most promising candidates for developing new types of memory, i.e., magnetic RAM (MRAM) for minimization and lowering power

consumption. The Mn_2 -based inverse-Heusler antiferromagnetic compounds are suitable as an alternative for the so-called critical raw materials [7]. Ferromagnetic Mn-based Heusler compounds are special and attract much interest as candidates for all-optical switching [8], the single-spin localization [9], and spin gapless semiconductivity [10]. Among the Heusler Mn_2YZ compound failures are high magnetic anisotropy constant, Curie temperatures above room temperature, which limits their applications. The Mn-based Heusler compounds are used in recent device as shape memory compounds, topological insulators, etc. [11]. The Mn-based ferrimagnets systems present large variability of compensation temperatures. Specifically, Mn_2PtZ Heusler. Experimentally, several samples of Mn-based Heusler are treated with arc melting characterization technical. For more technical characterization information, consult the papers in the refs [11–14].

*Corresponding author, E-mail: djizer@yahoo.fr; djillali.bensaid@univ-aintemouchent.dz

The experimental synthesis shows that Mn_2PtCo and Mn_2PtV are unstable and decompose into two phases cubic and tetragonal phases. The aim of this work is to develop the properties of new Mn_2 -based ferromagnetic Heusler materials. The synthesis of the regular Heusler compound Mn_2PtV is possible from our results, and their electronic and magnetic properties could lead to advances in magnetic memory devices.

The paper is split into four main parts. In the first part, we present the details of our computational approach. Then, in Sect. 2, it will begin by outlining the types of materials predicted theoretically and we discuss how the equilibrium structures for our compound were determined and their different structural properties. Thirdly, we try to analyze and understand the electronic and magnetic properties in terms of structural stability.

2. Calculation details

The electronic and magnetic structures of our compounds were investigated by employing the full-potential linearized augmented-plane-wave (FP-LAPW) method [15] as implemented in Wien2k package provided by Blaha, Schwartz and coworkers [16–18]. One of the most used the generalized gradient approximation (GGA) functional in solid-state physics is the implementation of Perdew, Burke and Ernzerhof (PBE) [19], plus we use the Colombian interaction approach (Hubbard). The GGA + U approach was chosen to treat the quantum effects contributed by the strongly correlated d-electrons. The muffin tin radii (R_{MT}) were chosen to make sure nearly touching spheres and minimizing the interstitial space. $R_{\text{MT}} \times K_{\text{max}} = 7$ was used for the number of plane waves, and the expansion of the wave functions was set to $L_{\text{max}} = 10$ inside of the muffin tin spheres, while the charge density was Fourier expanded up to $G_{\text{max}} = 12a.u^{-1}$, where G_{max} is the largest vector in the Fourier expansion. A $13 \times 13 \times 13$ point mesh was used as a base for the integration in The Brillouin zone sampling. The energy convergence criterion was set to 10^{-5}Ry .

3. Results and discussion

3.1. Determination of the stability structural

The full Heusler structure has the lattice formula X_2YZ , where X and Y are transition metals and Z is a main-group element with a 2:1:1 stoichiometric. Generally, the X_2YZ compounds crystallize in the regular and inverse cubic structure (Fm $\bar{3}$ m, space group no. 225 and F $\bar{4}$ 3 m, space

group no. 216) with Cu_2MnAl (L2₁) and Hg_2CuTi (X_a-type) as prototype (see Figs. 1b, a), respectively [20–24]. The inverse-Heusler structure can be viewed as four interpenetrating fcc sublattices. The x atomics are placed in Wyckoff positions, $(1/2, 1/2, 1/2)$ and $(3/4, 3/4, 3/4)$, while the positions $4c(1/4, 1/4, 1/4)$ and $4d(0, 0, 0)$ are filled with Y and Z atoms. Unlike the Heusler regular structure, the X atoms are placed on the Wyckoff position $8c(1/4, 1/4, 1/4)$, Y situate on $4a(0, 0, 0)$ and Z on $4b(1/2, 1/2, 1/2)$.

The axes of the cubic cells may be lengthened or compressed to get tetragonal derivative phases. The relation that links the parameters of the unit cell between the cubic and tetragonal phase is $c_{\text{tet}} = c_{\text{cub}}$ and $c_{\text{cub}} = \sqrt{2}a_{\text{tet}}$ [25]. A tetragonal distortion is observed for Mn_2YZ compounds crystallizing in the regular and inverse Heusler structure.

The regular tetragonal cell I4/mmm (space group no. 139) is derived from the L2₁ full Heusler structure. In this structure, the Mn atoms occupy the Wyckoff position $4d(0, 1/2, 1/4)$, the Y and the Z atoms locate at $2b(0, 0, 1/2)$ and $2a(0, 0, 0)$, respectively. The inverse tetragonal cell I4m2, space group no. 119, derived from the X_a-type inverse Heusler structure, the first Mn atom is located at the Wyckoff position $2b(0, 0, 1/2)$, while the second Mn atom and the Y atom are placed at the Wyckoff position $4d(0, 1/2, 1/4)$. Finally, the Z atom occupies the $2a(0, 0, 0)$ position.

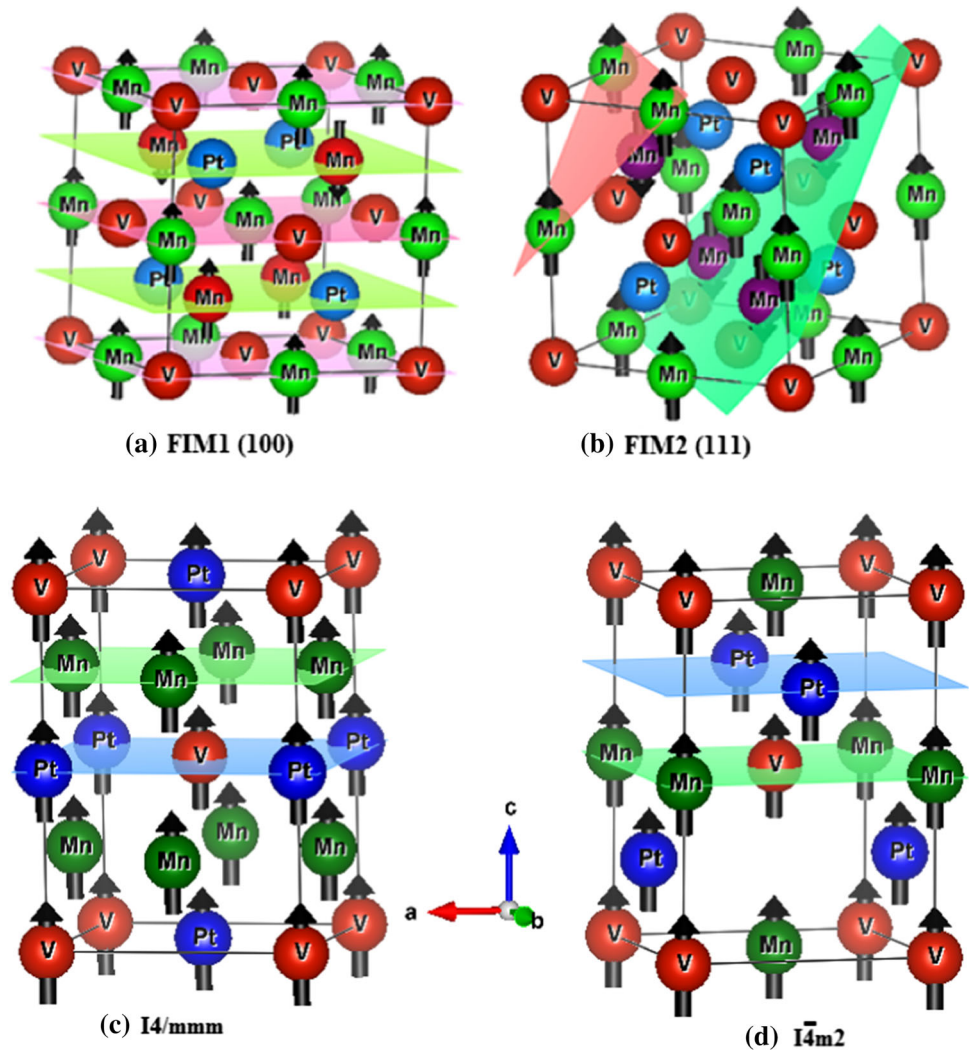
The first figure presents the two regular and inverse structures with their tetragonal distortions. We present in Fig. 2 the different magnetic configurations, the magnetic moments oriented are schematized by arrows and the lattice planes of the parallel magnetic moments are indicated by colored areas. In the ferrimagnetic (FIM) state of F $\bar{4}$ 3 m phase, we chose two configurations:

1. Firstly (FIM1), the moment of V(Co) atom is considered to be anti-parallel to the Mn atoms (both moments of Mn1 and Mn2 atoms are parallel to each other, in the plane family (100), see Fig. 1a).
2. Another configuration magnetic (FIM2) is that where moments of Mn1 and Mn2 are anti-parallel to each other and the moment of V(Co) is parallel to Mn2 (the moments are represented in the plane family (100), see Fig. 1b).

The structural stability of our Heusler compounds is determined by their formation energies. The formation energy of inverse-Heusler compound X_2YZ is defined as
$$\Delta E(\text{X}_2\text{YZ}) = E(\text{X}_2\text{YZ}) - 2E(\text{X}) - E(\text{Y}) - E(\text{Z}) \quad (1)$$

The formation energy for difference between the L2₁ and the X_a structure is given by the relation

Fig. 1 AF configurations in an fcc lattice. (a) FIM1 state with the parallel aligned magnetic moments in (001) plane. (b) FIM2 state with the parallel aligned magnetic moments in (111) plane. Designs are created with VESTA [140]



$$\Delta E_{RI} = \Delta E_{L21} - \Delta E_{Xa} \quad (2)$$

where $E(X)$ is the total energy of the ground state structure of element X .

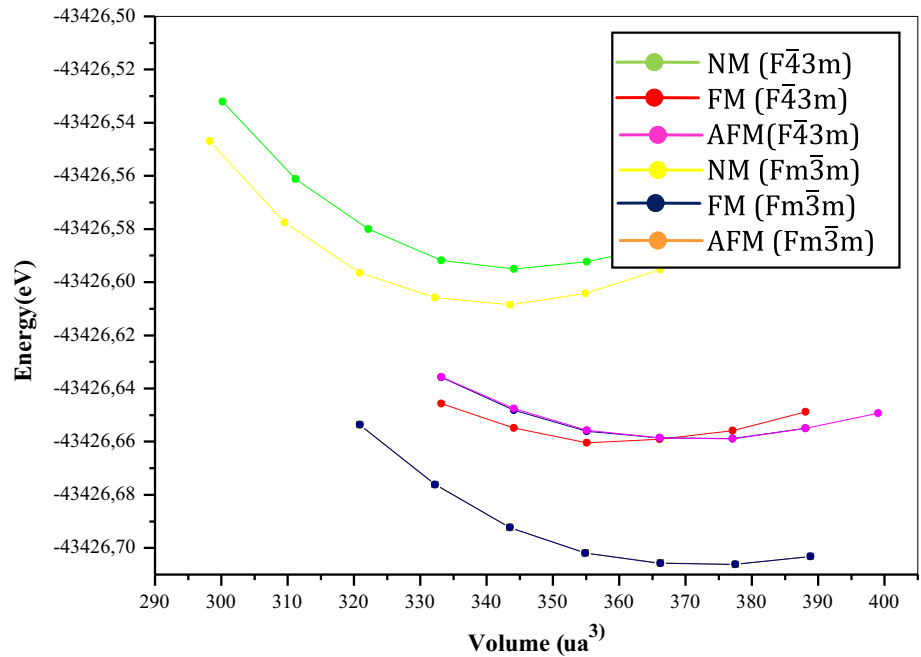
We found the $E_f(L21) < E_f(Xa)$, which implies that the synthesis of the regular phase is more realizable than the inverse phase, however, the formation energy is positive (≈ 34 and 176 meV/f.u for Mn_2PtZ ($Z = \text{VandCo}$)) indicating that phase segregation will occur. Among the parameters that show the material stability, its formation energy, the negative formation energy indicates that the crystal can exist stably.

The thermodynamic stability in the ground state requires at least two necessary and sufficient conditions. Firstly, a negative value of the formation energy contains information about the possible decomposition into the elemental constituents of a compound. Secondly, the energy value at the convex hull. Reference [26] provides details on the relationship between these two criteria. The connection between these two energies is given by the following

mathematical relation $E_{\text{hull}} + \Delta E_{\text{HD}} = \Delta E_{\text{for}}$. To determine E_{hull} , we use the grand canonical linear programming (GCLP) on the OQMD website [27]. Mn_2PtV is predicted to lie above the convex hull with a mixture of phases $MnPt-MnV$, the $\Delta E_{\text{HD}} = 0.018\text{eV/atom}$. Since the thermodynamic stability at 0 K is related to the convex hull distance (on the convex hull) by the condition $\Delta E_{\text{HD}} = 0$, the convex hull distance found in our compound is small and even lower than the empirical threshold values were predicted by Jianhua Ma et al. (52 meV / atom) [28]. It indicates that our compound will likely synthesize by equilibrium processing.

The curve $E-V$ for different structural phases and magnetic configurations of our compounds is presented in Fig. 2, in energetically plan, the ferromagnetic order is more stable for Mn_2PtV , with equilibrium theoretical lattice parameter equal to $a_{\text{eq}} = 6.0442\text{\AA}$, comparing our results with the data founded in the literature immediately indicates a very good agreement. The transition

Fig. 2 The variation in the calculated total energies of Mn_2PtV with full-Heusler $L2_1$ structure and inverse-Heusler X_a -type structure as a function of the lattice constant in ferromagnetic, antiferromagnetic and nonmagnetic states



temperature, TM, is connected by the relative energy change between the cubic and tetragonal phases $\Delta E_{\text{cub-tet}}$. Our results give 987.48 K and 2273.2 K for Mn_2PtZ ($Z = \text{VandCo}$), respectively. Unfortunately, we do not have theoretical results concerning the compressibility module and their derivative to compare them.

3.2. Electronic properties

In the context of this paper, the electronic band structure calculation is made along the directions of high symmetry of the Brillouin zone for the most stable structural phase and magnetic order, to understand the electronic properties of the Heusler alloy Mn_2PtZ ($Z = \text{VandCo}$). The structure band of the spin-resolved for the pure Mn_2PtV compound is calculated under the GGA. We noticed that the band structures are very similar and that there is no gap in the minority bands (the figure is not shown here). The band structure analysis for both Heusler alloys (Mn_2PtV and Mn_2PtCo) proves that the GGA approach is insufficient to show the half metallicity, because the minority bands around the level Fermi has a metallic nature.

The majority structure band rarely participates in the density of state, at level Fermi appearing highly dispersed bands. The presence 5d state of Pt leads to close the gap in the minority channel and consequently will destroy the half metallicity. However, the spin polarization remains important ($\approx 63\%$) for the perfect $L2_1$ structure of Mn_2PtV . According to Fig. 3, we notice the same reasoning for Mn_2PtCo but with a spin polarization of 91%. The

metallic character is observed in the minority channel due to the overlap between the bands energy and the absent band gap around the Fermi level.

Experimentally, the existence of half metallic in these two Heusler alloys (Mn_2PtV and Mn_2PtCo) has not yet proven, because the spin polarization does not equal 100%. We find that this loss of half metallic character caused to the DFT theory and the real structure of compound which is not perfectly ordered. The disorder mechanism or the temperature effect creates supplementary states in the minority band gap which destroy the half metallicity.

To explain the saturation magnetization found experimentally in some heusler compounds, it was necessary to include on-site correlations in the calculations. That is, go beyond GGA. Mn_2PtZ ($Z = \text{VandCo}$) is generally considered to be a compound with a magnetic moment located on the 3d orbital of the element Mn, where the electron-electron correlations can play an important role. This type of correlation was treated using the GGA + U formalism, where U is the Hubbard term and stands the electron-electron Coulomb repulsion energy for electrons occupying the same orbital. We have introduced a Coulomb interaction equal 3eV. In this formalism, we only test the Mn_2PtV compound for order to get a clear vision to the half metallicity. A look at Fig. 4, we can immediately say that the addition of the correlation term to a major significant effect on minority states where an opening appears at the fermi level that gives the half metallicity of our compound.

The density of states (DOS) as a function of energy for the spin-up and spin-down states of Mn_2PtV is illustrated in Fig. 3. The spin-up states band has a larger population of

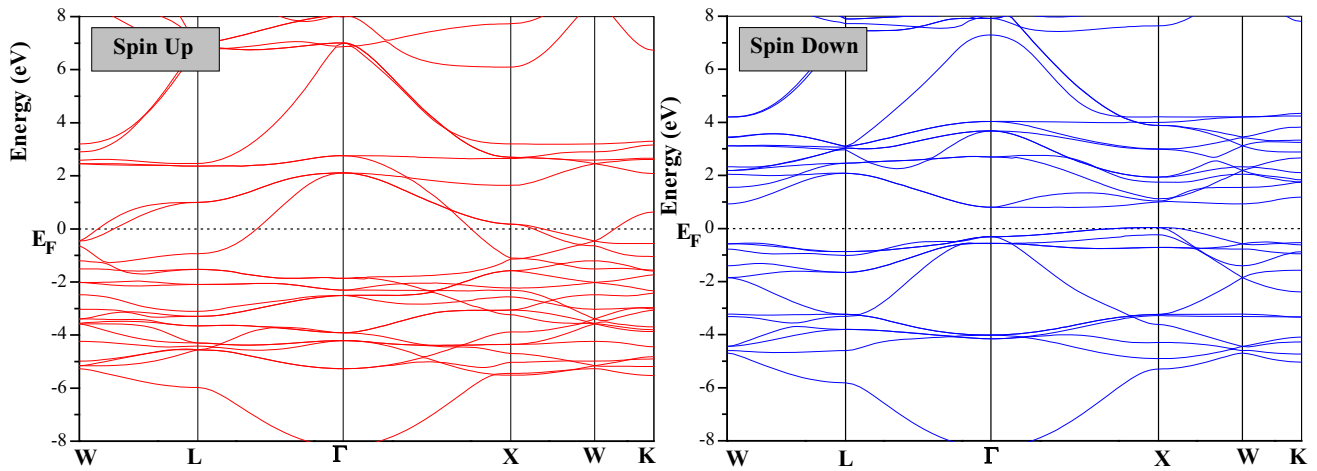


Fig. 3 The spin-polarized band structures for the L_{21} structure of the Mn_2PtV compound in FM phase within GGA + U approach

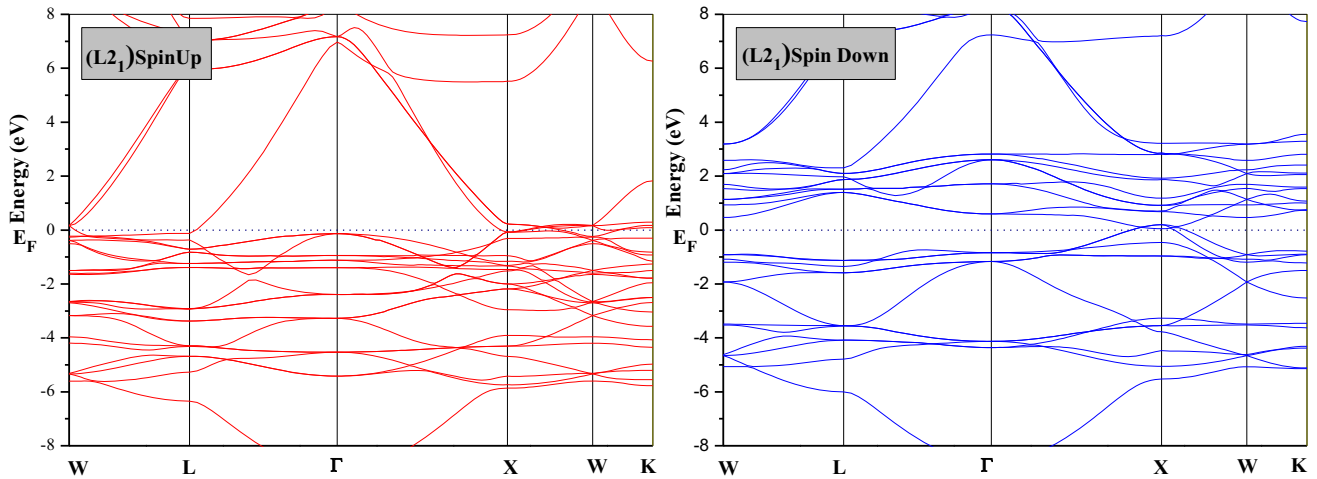


Fig. 4 The band structure of Mn_2PtCo with ferromagnetic full-Heusler L_{21} structure

electrons that the spin-down states band has a smaller population, leading to a spin polarization less than unity. The Mn_2PtV compound has an indirect band gap for the spin-down band, where the minima conduction band is located at the Γ -point and the maximum valence band touches the X-point, shown in Fig. 3. The magnetism is ferromagnetic with total magnetic moment $4.87 \mu_B$, where the Mn atoms on the two different sublattices are aligned, with same magnetic moments.

For Mn_2PtCo , one can clearly see at the level of the minority band structure the appearance of a gap along the path $W \rightarrow L \rightarrow \Gamma$. Then, at the point of high symmetry X, we can observe that the valence band slightly exceeds the level of fermi which implies the destruction of the half metallic behavior (see Fig. 4).

Figure 5a shows the spin polarized density of states total and projected by atom of Mn_2PtV in the GGA approach. The density of states has been projected in the range of -

9 eV to 9 eV. Our calculations show very small DOS at the Fermi level in spin down, which decreases polarization by 30%. We start the energy order of the atomic orbitals by Mn-3d states forming a narrow band below the Fermi level, followed by Pt-5d in the majority channel at valence band. More, we observed two acute peaks located at -4.2 and -1.4 eV, respectively, because of the superexchange ferromagnetic interaction. In the conduction band, the order of states d is inverted, V-3d, followed by Mn-3d in the majority channel.

In Fig. 5b, we present the total density of states (TDOS) (black lines) and partial density of states (PDOS) projected on to Pt-5d (blue lines), V-3d (red lines) and Mn-3d (magenta lines) in ferromagnetic order with GGA + U approach.

The comparison of the DOS obtained with GGA and GGA + U leads to say the bands almost similar, the major difference is the density of peaks and the appearance of a

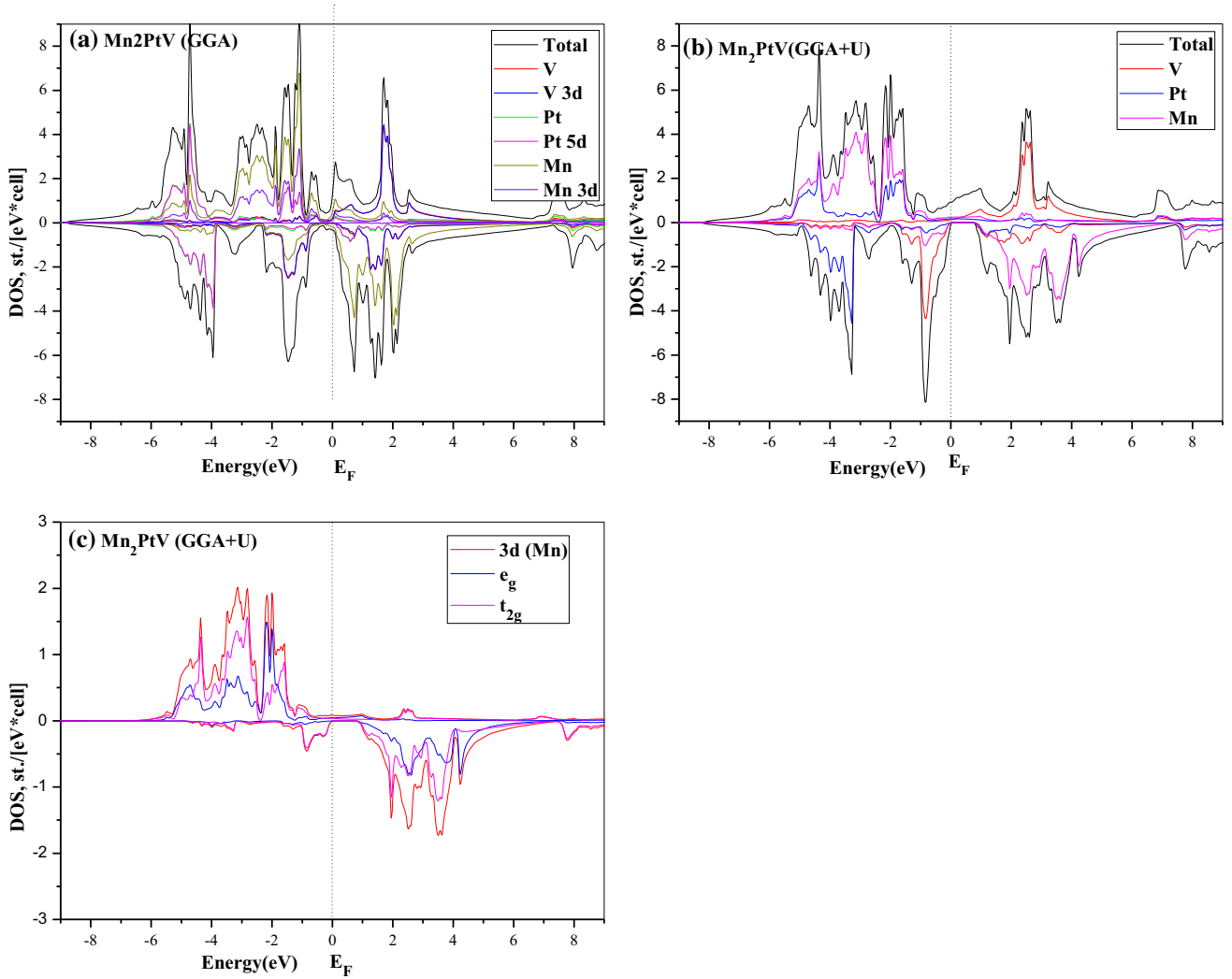


Fig. 5 Total and partial density of states for ferromagnetic Mn₂PtV calculated with (a) GGA, (b) GGA + U and (c) Symmetry-resolved local DOS for Mn 3d states

gap at fermi level in minority band. The 5d Pt bands in the valence band shift to the fermi level, contrarily of the 3d V bands shifts with 0.3 eV to the low energy.

The peak at 1.8 eV crawl at the $\sim E_g$ eV, approximately, to the high energy in spin up. The displacement of these bands is affected on the value of the total magnetic moment.

Figure 5c shows the symmetry-resolved local DOS for the Mn atom in the L₂₁ ferromagnetic (FM) configurations. The peaks in the PDOS of Mn are well separated on the energy scale. Among the consequences of the hybridization of the Mn atoms on the 8c site (which has a tetrahedral coordination with the neighboring atoms) is the creation of a gap in the minority channel. Because of the crystal field, 3d Mn orbitals interact with each other, the state d is divided into double-degenerated bonding e_g with low

energy and triple-degenerated bonding t_{2g} with high energy. It is clear that the hybridization bonding states e_g and t_{2g} are mainly formed by Mn-3d state which contribute to the TDOS in the energy region from - 5.4 to - 1.25 eV (1.05–4.8 eV) for up spin channel (down spin channel), respectively (see Fig. 5c).

We have found that the origin schematic construction of the difference in the minority spin band in the Mn₂PtV compound depends on the following construction. The Fermi level is found between the two antibonding e_g and t_{2g} of 3d Mn orbitals. Thus, a band gap opens in the minority spin band. The module of the gap is related only to the Mn–Mn interactions.

The state density analysis of Mn₂PtCo is displayed in Fig. 6, the spin-up state band contains a larger electron

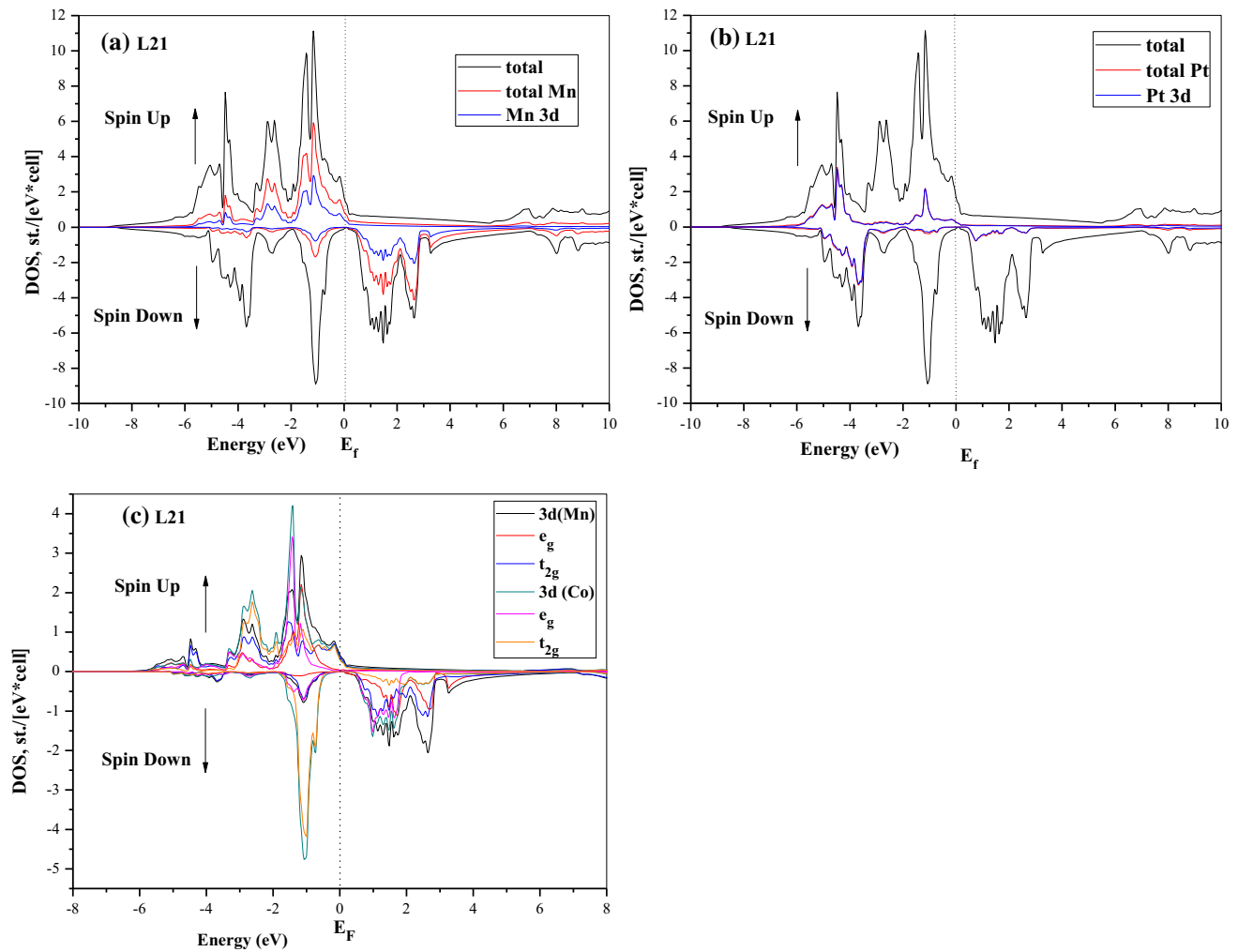


Fig. 6 Total and partial density of states for ferromagnetic Mn_2PtCo calculated with (a) Mn, (b) Pt and (c) Co 3d states

population than the spin-down state band, which leads to a spin polarization < 1 .

The spectral mass is of the order $0.01\text{eV} / \text{cell}$ in the minority band for the three elements of this material which gives a 91% spin polarization at the Fermi level.

The contribution of the electronic states differs from one atom to another, so we can draw some remarks:

Near Fermi level:

- In the energy range -5 to -3 eV, the Pt contributes more than the other elements.
- The contribution of the element Mn is much more dominant than the other elements, in a range of energies between -5.5 eV to E_F for the valence band, this contribution is accompanied by an average contribution of the elements Co and Pt.

In addition, we observed two sharp peaks located, respectively, at -4.5 and -1.17 eV, due to the ferromagnetic super exchange interaction between the two

localized magnetic moments of Mn and Pt. We observe a sharp peak of 6.36 eV/cell near fermi level due to a large hybridization between the d states of Mn and Pt.

3.3. Magnetic properties

For testing the half metallicity behavior of alloys, it is important to measure the saturation magnetization of these alloys. If the compound is half metallic, its saturation magnetization should follow the behavior of Slater-Pauling. The magnetic moment for the investigated compound is almost exclusively localized on the Mn atom. In the case of our Full-Heusler alloy Mn_2PtV , each Pt atom has eight Mn atoms as first neighbors, therefore, the hybridization effect becomes very important and stabilizes the Mn spin moment to $3\mu_B$ and corrected the total spin magnetic moment M_t , this last is correlated to the total number of valence electrons Z_t by the relation $M_t = Z_t - 24$. The total magnetic moment located mostly at the Mn atom, its

Table 1 The lattice parameters a , bulk modulus, c/a ratio corresponding tetragonal structures, $C_{t/c}$ relative volume change between the cubic and tetragonal phase, E_{coh} cohesion energy and ΔE_{FM} total energy differences to the FM state of Mn_2PtZ ($Z = \text{VandCo}$), compound

Mn_2PtV	$a(\text{\AA})$	c/a	$B(\text{GPa})$	B'	$C_{t/c}$	$\Delta E_{\text{cub-tet}}(\text{Ry})$	$\Delta E_{\text{FM}}(\text{Ry})$	$E_{\text{coh}}(\text{Ry})$
F $\bar{4}3m$								
NM	5.894		243.68	4.16			0.06.508	
FM	5.976		179.6	5.14				
FIM1	6.0315	1.00	155.38	4.09				
FIM2	6.0356		153.5	3.46				
Theory	6.06 ^a							
Fm $\bar{3}m$								
NM	5.871		255.6	4.58				
FM	6.0442		160.27	4.92				
GGA + U(FM)	6.20		136.08	4.25			0.098098	2.483
FIM	6.0444		159.8	4.97				
Tetragonal								
I $\bar{4}m2$	4.0647	1.5142	263.85	4.59	-7.90	0.085128		
Mn_2PtCo								
F $\bar{4}3m$								
NM	5.775		140.64	4.33				
FM	5.955		264.7	4.77			0.00003	
FIM	5.946		159.96	4.85		0.196		
Fm $\bar{3}m$								
NM	5.797		247.33	4.08				
FM	5.998		200.58	2.57			0.039246	13.0
FIM	5.996		191.57	4.12				
Theory	6.00 ^a							

^aRef. [14]

estimated value $4.87 \mu_B$ in ferromagnetic (FM). Our result is close to the value obtained by stevano sanvito and all [14]. We find that our magnetic moment value is deviating to the theoretical value, due to the possible stoichiometric deviation (Table 1).

According to Slater-Pauling rule, the magnetic moment depends on the number of valence electrons Z_t and since $Z_t = 29$ for our compound so the magnetic moment equal $5 \mu_B$. Our result with GGA + U is closed to the ideal value (deviation 0.26%).

Table 2 shows the total and atomic magnetic moments of Mn_2PtV , we observe that the magnetic moment resides almost exclusively in the Mn atom and originates from the d electrons as expected with little contribution of Pt atom.

For the compound Mn_2PtCo , we found a total magnetic moment value equal to $8.22 \mu_B$ for the ferromagnetic configuration. This value is deviated by 8.66% from the theoretical value of the Slater-Pauling rule. For the ferrimagnetic (FIM) configuration, we found a value equal to $0.754 \mu_B$. Our result is in good agreement with the value found by stevano & al [14] (see Table 2). We notice that most of the contribution in the total magnetic moment is

due to the manganese element, but a negligible contribution to the platinum atom.

The application of the GGA + U approach in the stable structure fm $\bar{3}m$ in the FM configuration, our values obtained coincide with the Slater-Pauling rule because we found $5 \mu_B$ and $9 \mu_B$ for Mn_2PtV and Mn_2PtCo , respectively.

The actuality of spintronic technology is to use compounds that have specific properties such as high spin polarization and high Curie temperature. The half metallic Heusler family is a preferred choice for magnetic tunnel junctions (MTJ), spin-transfer torque MRAM (STT) and spin-FET Datta-Das. The Curie temperature is important aspect of application for spin injectors, due to the strong orbital interactions between 3d Mn -5d Pt and 3dMn₁-3dM₂ on different sublattices. Generally, the high Curie temperature is the desirable property in half metallic ferromagnet compounds.

We can estimate the Curie temperature in the standard mean-field approximation by the following equation [29]:

$$T_c = \frac{2}{3K_B} \sum_{i \neq j} J_{ij} \quad (3)$$

Table 2 Atomic magnetic moments (μ_B) in Mn_2PtZ ($Z = \text{VandCo}$), compound, $M_{\text{Tot}}(\mu_B)$ is the total magnetization, P spin polarization and Curie temperature

Mn_2PtV $F\bar{4}3m$	M_{Tot}	$M(\text{Mn1})$	$M(\text{Mn2})$	$M(\text{Pt})$	$M(\text{V})$	P%	T_c (K)
FM	4.656	1.166	3.1371	0.28	-0.115		503.03
Theory	4.87 ^a					67 ^a	
$Fm\bar{3}m$							
FM	4.699	2.993		0.414	-1.581	63.16	
FIM1	4.874	3.053		0.419	-1.559		
FM(GGA + U)	4.987	3.73		0.232	-2.212	100	758.24
Mn_2PtCo					$M(\text{Co})$		
$F\bar{4}3m$							
FM	8.224	2.84	2.93	0.43	1.774	91	157.72
FIM2	0.754	-2.973	3.183	0.25	0.2		
$Fm\bar{3}m$							
FM	9.012	3.325		0.488	1.617		206.3
Theory	9.04(1.13 ^a)					86(0.0 ^a)	

^aRef [14]

where J_{ij} is the exchange interaction and K_B is the Boltzmann constant ($K_B = 1.38064852 \times 10^{-23} \text{J/K}$).

Our calculation result for the Curie temperature of the ferromagnetic compound Mn_2PtV with the mean field approximation (MFA) is 758 K, we find that this value is in good agreement with other theoretical values predicted for similar compounds.

We noticed that the T_c is reduced during the transition to a weakly symmetric structure for Mn_2PtCo . This significant reduction occurs due to small interaction between the Mn (4d) -Mn (4b) site, which can indicate an unstable magnetic ground state.

We observed that the Curie temperature in our work was below room temperature ($T_c = 206.3 \text{K for } X_a \text{ structure}$) for cubic phases.

The main drawback of Heuslers compounds is that their Curie temperature is below room temperature, making them unusable for spintronics applications.

4. Conclusions

As summarized, this ab-initio study based on the determination and the understanding of the electronic and magnetic properties of Mn_2PtZ ($VandCo$) compounds. Through analysis and extrapolation of our results, we draw some important conclusions. Within the GGA approach cannot demonstrate the half metallicity because of the absence of the gap in minority spin band. However, to appear a gap in the minority spin channel, we must take into account the strong correlations of the d-Mn states. Thanks to the application of the Hubbard correlations, a

gap opened by a displacement of the bands e.g. Our recent calculation employing the Hubbard U has shown that Mn_2PtV is susceptible of being a half metal with a minority gap equal 0.775 eV and $\approx 5\mu_B$ for total spin magnetic moment. We confirmed that the Mn_2PtCo alloy is more stable in the regular $L2_1$ heusler structure at the ferromagnetic phase.

It's clear that the majority and minority electrons (spin-up and down) have a metallic character with a polarization equal 91%.

We have reported a total magnetic moment about $\approx 9\mu_B$ for ferromagnetic order.

The adding of four valence electrons to the 4a site by replacing vanadium with cobalt effecting a change in the total magnetic moment and the spectral mass at the fermi level and consequently the polarization.

We point out that our bibliographic research tells me that no study was done on this compound, which leads to confirm that we can take this study as a basis for future research.

References

- [1] S Datta and B Das *Appl. Phys. Lett.* **56** 665 (1990)
- [2] K A Kilian and R H Victora *J. Appl. Phys.* **87** 7064 (2000)
- [3] C T Tanaka J Nowak and J S Moodera *J. Appl. Phys.* **86** 6239 (1999)
- [4] J A Caballero et al. *J. Vac. Sci. Technol.* **A16** 1801 (1998)
- [5] C Hordequin J P Nozieres and J Pierre *J. Magn. Magn. Mater.* **183** 225 (1998)
- [6] S Chadov, T Graf, K Chadova, X Dai, F Casper and G H Fecher and C Felser *Phys Rev. Lett.* **107** 047202 (2011)

- [7] European Commission *Report on critical raw materials for the EU – Report of the Ad hoc Working Group on defining critical raw materials*. (Brussels, Belgium: European Commission) (2014)
- [8] C D Stanciu, F Hansteen, A V Kimel, A Kirilyuk, A Tsukamoto and A Itoh and Th Rasing *Phys Rev. Lett.* **99** 047601 (2007)
- [9] S Chadov and J Kiss and C Felser *Adv Funct. Mater.* **23** 832 (2013)
- [10] S Ouardi, G H Fecher and C Felser and J Kubler *Phys Rev. Lett* **110** 100401 (2013)
- [11] J Winterlik et al. *Adv. Mater.* **24** 6283 (2012)
- [12] C J Palmstrøm. **62** 371 (2016)
- [13] E Michelle. Jamer, Phd thesis (The Faculty of the College of Science of Northeastern University) (2015)
- [14] S Sanvito and C Oses JXue, ATiwari, M Zic, TArcher, PTozman, M Venkatesan, M Coey *S Curtarolo Sci. Adv.* **3** e1602241 (2017)
- [15] P Blaha, K Schwarz, G K H Madsen, D Kvasnicka and J Luitz WIEN2k, An Augmented Plane Wave C Local Orbitals Program for Calculating Crystal Properties ed K Schwarz (Wien: Technical Universitaet Wien) (2001)
- [16] P Blaha, K Schwarz, P Sorantin and S B Tricky *Comput. Phys. Commun* **59** 399 (1990)
- [17] P Blaha, K Schwarz, G K H Madsen, D Kvasnicka and J Luitz *WIEN2k, An Augmented Plane Wave + Local Orbitals Program for Calculating Crystal Properties*. (Austria: Techn. Universitat Wien) (2001)
- [18] K Schwarz, P Blaha and G K H Madsen *Comput. Phys. Commun.* **147** 71 (2002)
- [19] J P Perdew, K Burke and M Ernzerhof *Phys. Rev. Lett.* **77** 3865 (1996)
- [20] F Heusler, W Starck and E Haupt *Verh. DPG* **5** 220 (1903)
- [21] F Heusler *Verh. DPG* **5** 219 (1903)
- [22] O Heusler Kristallstruktur und Ferromagnetismus der Mangan-Aluminium-Kupferlegierungen) (German *Ann. Phys* **411** 155–201 (1934)
- [23] A J Bradley and J W Rodgers *Proc. R. Soc. A* **144** 340 (1934)
- [24] T Graf, S Parkin and C Felser *IEEE Trans. Mag.* **47** 367 (2011)
- [25] L Wollmann and S Chadov J Kübler and C Felser *Phys Rev. B* **92** 064417 (2015)
- [26] Jianhua Ma et al *Physical Review B* **95** 2 024411 (2017)
- [27] The Open Quantum Materials Database, <http://oqmd.org/analysis/gcpl>
- [28] J Ma, J He, D Mazumdar, K Munira, S Keshavarz and T Lovorn C Wolverton A W Ghosh, and W H Butler *Physical Review B* **98** 094410 (2018)
- [29] A I Liechtenstein and M I Katsnelson P V Antropov and A V Gubanov *J Magn. Materials* **67** 65 (1987)
- [30] K Momma et F izumi *J. Appl. Crystallogr.* **44** 1272 (2011)

Publisher's Note Springer Nature remains neutral with regard to jurisdictional claims in published maps and institutional affiliations.